Electrochimica Acta 56 (2011) 9056–9063

Contents lists available at ScienceDirect

Electrochimica Acta

journal homepage: www.elsevier.com/locate/electacta

Chitosan–Fe_3O_4 nanocomposite based electrochemical sensors for the determination of bisphenol A

Chunmei Yu, Lili Gou, Xiaohui Zhou, Ning Bao, Haiying Gu*

Institute of Analytical Chemistry for Life Science, School of Public Health, Nantong University, Nantong 226019, PR China

ARTICLE INFO

Article history:
Received 1 March 2011
Received in revised form 27 May 2011
Accepted 28 May 2011
Available online 23 July 2011

Keywords:
Chitosan–Fe_3O_4 nanocomposite
Bisphenol A
Electrochemical sensor
Amperometric determination

ABSTRACT

This paper reports the application of chitosan–Fe_3O_4 (CS–Fe_3O_4) nanocomposite modified glassy carbon electrodes for the amperometric determination of bisphenol A (BPA). We observed that the CS–Fe_3O_4 nanocomposite could remarkably enhance the current response and decrease its oxidation overpotential in the electrochemical detection. Experimental parameters, such as the amount of the CS–Fe_3O_4, the accumulation potential and time, the pH value of buffer solution etc. were optimized. Under the optimized conditions, the oxidation peak current was proportional to BPA concentration in the range between 5.0×10^{-8} and 3.0×10^{-5} mol dm^{-3} with the correlation coefficient of 0.9992 and the limit of detection of 8.0×10^{-9} mol dm^{-3} (S/N = 3). The proposed sensors were successfully employed to determine BPA in real plastic products and the recoveries were between 92.0% and 06.2%. This strategy might open more opportunities for the electrochemical determination of BPA in practical applications. Additionally, the leaching studies of BPA on incubation time using the as-prepared modified electrode were successfully carried out.

1. Introduction

During the past few years, environmental chemists have been widely concerned about some substances as endocrine disrupting chemicals. Among them, bisphenol A (BPA) is highly suspected to act as an endocrine disruptor and used mainly in the broad production of epoxy resins, flame retardants and polycarbonate [1,2]. BPA is ubiquitous because it can be released into the environment from the food and drink packaging, the nursing bottle, food cans as well as beverage containers. More importantly, the releasing rate of BPA from the polymer matrix to the environment was determined to be increased by approximately 1000 folds when containers are aged [3]. BPA shows estrogenic potential both in vitro and in vivo [4] and also acute toxicity toward aquatic organisms [5] and human cultured cells [6]. In addition, BPA is postulated to cause reproductive disorders including decrease of sperm quality in humans, birth defects due to its fetal exposure and various kinds of cancers, such as prostate, testicular, and breast cancer [7]. Therefore, an easy and sensitive analytical method for the detection of BPA has become an essential issue in the environment monitoring.

Various analytical methods ranging from enzyme-linked immunosorbent assay (ELISA) [8] and chemiluminescence immunoassay [9] to chemical methods such as high-performance liquid chromatography (HPLC) [10], and more sophisticated liquid chromatography–mass spectrometry (LC–MS) [11], gas chromatography–mass spectrometry (GC–MS) [12,13] have been reported for determination of BPA. However, normally these methods are expensive and time-consuming, requiring skilled operators and extraction steps [14,15]. By comparison, electrochemical sensors are rapid and low cost. Furthermore, they have extra advantages of high sensitivity, simple operation, the potential for miniaturization, and the possibility of in situ analysis [16]. Electrochemical studies of alkyl phenols with estrogenic properties have been recently reported. The voltammetric behavior of xenoestrogens 4-nonylphenol (NP) and BPA at a platinum electrode has been compared with that of β-estradiol and other natural hormones [17]. Moreover, carbon fiber electrodes were used to for the electrochemical removal of BPA [18]. Although BPA is electrochemically active, the direct determination of BPA using bare electrode is not applicable because the responses of BPA at traditional electrochemical sensor are very poor [19]. It has been reported that the oxidation peak current of BPA was small at the bare GCE compared with the CNT-GCE [20]. To increase the sensitivity and selectivity for the detection of BPA, various modified electrode such as ITO [21], thionine-tyrosinase [22] and cobalt phthalocyanine [23] modified carbon paste electrode, Mg–Al layered double hydroxide modified GCE [24], poly(thionine)-tyrosinase modified GCE [25], Ni(II) tetraamino metallophthalocyanine polymer modified Au electrode [26] have been developed.

* Corresponding author. Tel.: +86 513 8501 5417; fax: +86 513 8501 5417.
E-mail addresses: hygu@ntu.edu.cn, guhy99@21cn.com (H. Gu).

0013-4686/$ – see front matter © 2011 Elsevier Ltd. All rights reserved.
doi:10.1016/j.electacta.2011.05.135

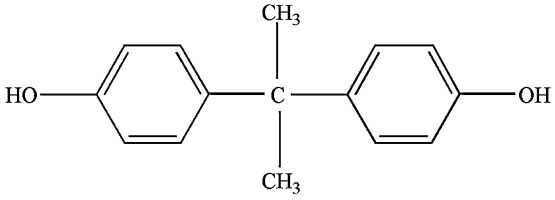

Fig. 1. The chemical structure of BPA.

To date, nanomaterials, such as CoTe quantum dots [27], mesoporous silica [28], gold nanoparticles [29] and multiwalled carbon nanotubes [20,30], etc. have been applied for the determination of BPA. Among lots of nanoparticles (NPs), Fe_3O_4 magnetic NPs have attracted extensive attentions due to their unique multifunctional properties such as small sizes, the superparamagnetism, the biocompatibility and the low toxicity, etc. However, the tendency of aggregation of NPs makes it impossible to disperse them into a suitable matrix for the enhancement of the stability. Chitosan, as a polyaminosaccharide with unique biological and chemical properties, has been widely used in the fields of medicine, pharmacy and biotechnology. In particular, because of its desirable properties, chitosan has been combined with Fe_3O_4 NPs in electrochemical sensing platforms. Wang et al. [31] developed a tyrosinase biosensor based on Fe_3O_4 NPs-chitosan nanocomposite to detect phenolic compounds such as catechol and phenol. Chang and Chen [32] applied the monodisperse chitosan-bound Fe_3O_4 NPs as a novel magnetic nano-adsorbent for the removal of heavy metal ions. Their results indicated that the large surface area of Fe_3O_4 NPs and the porous morphology of chitosan could have high accumulation efficiency.

Herein we report the application of the Fe_3O_4 NPs modified electrodes for the determination of BPA. Fe_3O_4 NPs were dispersed into chitosan (CS) solution, resulting in a stable and homogeneous CS–Fe_3O_4 suspension. The nanocomposite was then used to fabricate CS–Fe_3O_4/GCE for the determination of BPA. We observed that the oxidation peak height of BPA was significantly increased at the CS–Fe_3O_4/GCE with an enhanced sensitivity for BPA determination comparing with the bare GCE. The essential factors on electrochemical oxidation of BPA were investigated in details. In addition, the proposed method was applied to detect BPA in real plastic samples. Finally, the proposed approach was applied for the leaching studies of BPA on incubation time.

2. Experimental

2.1. Reagents

Bisphenol A (BPA) was purchased from Sigma Co. (USA). Its chemical structure is presented in Fig. 1. 0.1 mol dm^{-3} BPA stock solution was prepared with ethanol and kept in refrigerator at 4 °C. Working solutions were freshly prepared before use by diluting the stock solution. $FeCl_2{\cdot}4H_2O$ and $FeCl_3{\cdot}6H_2O$ were purchased from Shanghai No.1 Reagent Factory. Chitosan (90% deacetylation) was from Sinopharm Chemical Reagent Co., Ltd. The phosphate buffer solution (PBS, 0.1 mol dm^{-3}) was prepared from Na_2HPO_4 and NaH_2PO_4, and the pH adjusting was regulated with H_3PO_4 and NaOH. Other chemicals were of analytical grade. All solutions were prepared with twice-distilled water.

2.2. Apparatus and measurements

All electrochemical measurements were performed with a CHI 660 electrochemical workstation (CH Instruments Co., USA). The electrochemical cell consisted of a three-electrode system with a modified glassy carbon electrode (GCE) (4 mm in diameter) as a working electrode, a platinum wire as a counter electrode and a saturated calomel electrode (SCE) as a reference electrode. All potentials in this paper were referenced to the SCE. All solutions were deoxygenated by bubbling highly pure nitrogen for at least 15 min and a nitrogen atmosphere was maintained during the measurements. After a 150 s accumulation at the potential of −0.1 V, cyclic voltammograms were recorded in the potential range from 0.30 to 0.8 V with the scan rate of 100 mV s^{-1}. The differential pulse voltammetry was carried out with the parameters of increment potential, 0.005 V; pulse amplitude, 0.05 V; pulse width, 0.05 s; sample width, 0.0167 s; pulse period, 0.2 s; quiet time, 2 s. Each experimental point in the figures represents the average of five experiments carried out under the same conditions. The average particle size and morphology of the Fe_3O_4 nanoparticles was observed by a JEM-2010HR transmission electron microscope (TEM). X-ray diffraction (XRD) measurement was performed on a Philips D/Max-2500 diffractometer, using a monochromatized X-ray beam with nickel-filtered Cu Kα radiation with 4° min^{-1} scan rate. A continuous scan mode was used to collect 2θ data from 10° to 80°. X-ray photoelectron spectrum (XPS) was taken on Perkin-Elmer PHI 550 spectrometer (PHI Co., USA), equipped with the Al Kα X-ray radiation as the source for excitation at a pressure of below 10^{-9} Torr in the chamber. The analyzer pass energy was 50 eV and the step size was 0.1 eV. Electrochemical impedance spectroscopy (EIS) experiments were performed at a potential of 0.17 V within the frequency range from 10^{-2} to 10^5 Hz in 0.1 mol dm^{-3} KNO_3 containing 5.0 mmol dm^{-3} $Fe(CN)_6^{3-}$/$Fe(CN)_6^{4-}$ (1:1).

2.3. Preparation of CS–Fe_3O_4 nanocomposite

Fe_3O_4 NPs were synthesized according to reported method [33]. Chitosan was dissolved in 0.05 mol dm^{-3} acetate buffer to form 0.2 wt% solution and then filtered using a 0.45 mm syringe filter unit. The pH value was adjusted to 5.0 with NaOH solution. CS–Fe_3O_4 nanocomposite with various concentrations was obtained by dispersing different amount of Fe_3O_4 NPs in the 5 mL CS solution. The suspension was mixed by ultrasonic irradiation for 1 h. Finally, a viscous solution of CS with uniformly dispersed Fe_3O_4 NPs was obtained.

2.4. Fabrication of the modified electrode

Prior to modification, the bare GCE was firstly polished with abrasive paper and then with alumina slurry on microcloth pads, followed by rinsing with water and ethanol and briefly cleaning in an ultrasonic bath, then rinsed thoroughly in twice-distilled water and dried in air.

Typically, 10 μL of CS–Fe_3O_4 nanocomposite was dropped on the surface of the cleaned GCE with a microinjector. After the solvent was evaporated, the electrode surface was thoroughly rinsed with redistilled deionized water and dried in the air. The obtained electrode was noted as CS–Fe_3O_4/GCE. By the similar way, CS/GCE and Fe_3O_4/GCE were obtained by casting 10 μL CS and 10 μL Fe_3O_4 NPs on the GCE surface respectively. When not in use, the sensor was preserved at 4 °C in a refrigerator.

2.5. Sample preparation

Four kinds of plastic products (PVC drinking cup, nursing bottle, baby's nipple and food package) were purchased from a local supermarket. These samples were cut into small pieces and washed twice with redistilled water. Then the plastic products were treated as following process to obtain sample solutions. Plastic product pieces (1.00 g) and redistilled water (50 mL) were added into a beaker and sealed with aluminum foil. Then the sample was immersed in 70 °C

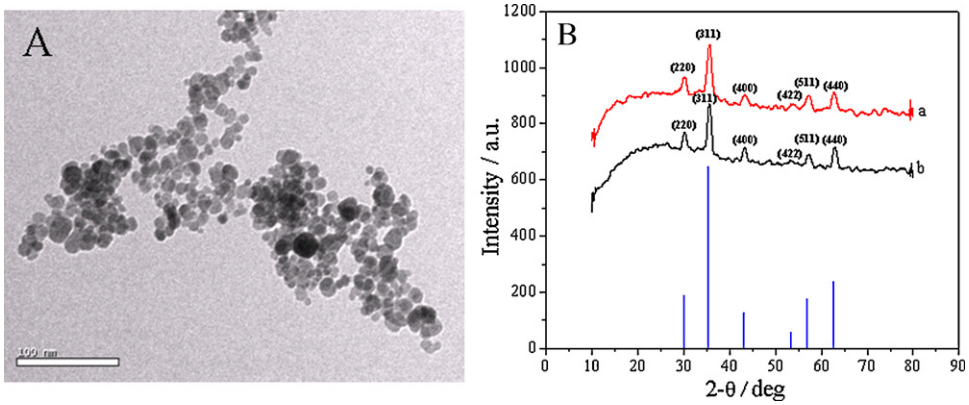

Fig. 2. (A) Transmission electron micrograph of Fe_3O_4 NPs. (B) X-ray diffraction patterns of (a) Fe_3O_4 NPs and (b) CS–Fe_3O_4 nanocomposite.

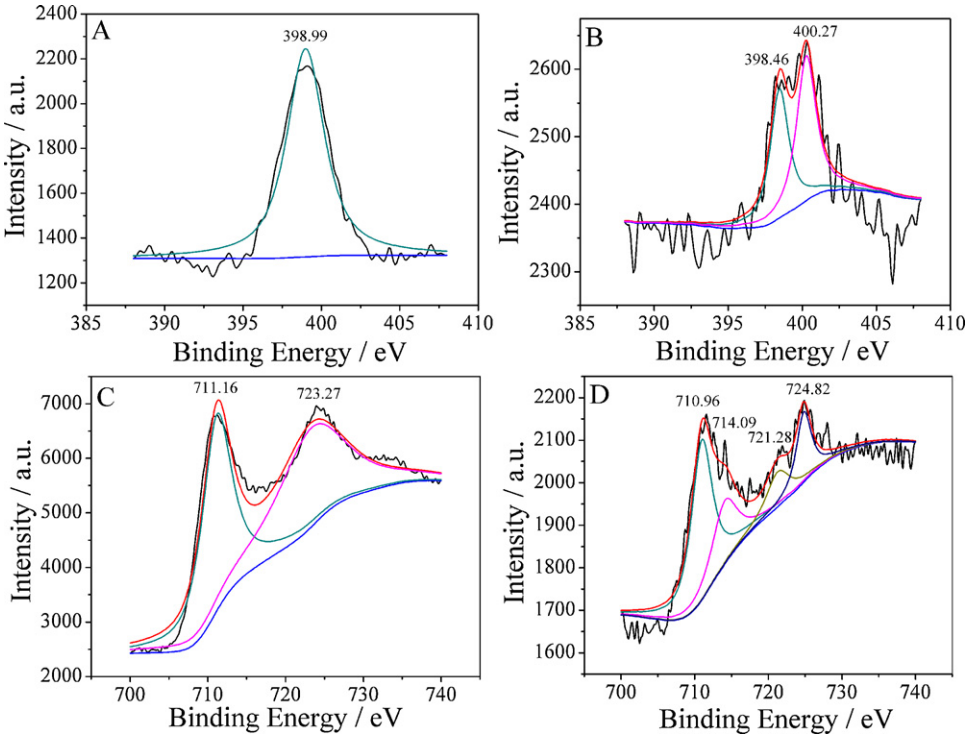

Fig. 3. XPS spectra of the N element in (A) CS and (B) CS–Fe_3O_4 nanocomposite, Fe element in (C) Fe_3O_4 NPs and (D) CS–Fe_3O_4 nanocomposite.

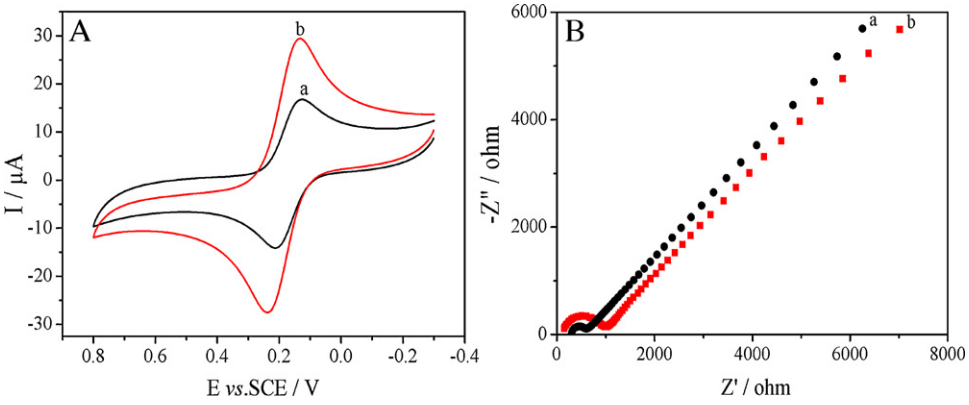

Fig. 4. (A) Cyclic voltammograms of 5.0 mmol dm^{-3} $K_3[Fe(CN)_6]$ at (a) bare GCE and (b) CS–Fe_3O_4/GCE in 0.1 mol dm^{-3} KNO_3 with scan rate 100 mV s^{-1}. (B) Nyquist plots obtained from impedance measurements in the presence of 5.0 mmol dm^{-3} $K_3[Fe(CN)_6]/K_4[Fe(CN)_6]$ (1:1) and 0.1 mol dm^{-3} KNO_3 solution for (a) GCE and (b) CS–Fe_3O_4/GCE.

constant temperature water bath for 48 h. After filtrated, the liquid phase was collected in a 50 mL volumetric flask and diluted to volume with redistilled water.

BPA leaching studies were carried out using PVC drinking cups as the model. 1.00 g product pieces were added into 50 mL redistilled water in a beaker and sealed with aluminum foil. The as-prepared samples were immersed in 40 °C constant temperature water bath for 6 days then increased to 55 °C to 18 days. Totally five sample solutions were prepared and one sample solution was taken out for analysis at regular intervals.

3. Results and discussion

3.1. Characterization of Fe_3O_4 NPs and CS–Fe_3O_4 nanocomposite

The TEM image (Fig. 2A) of Fe_3O_4 NPs indicates that the magnetite particles are nanocrystalline. The size of the spherical NPs varies from ~ 8 to ~15 nm with average particle size of ~12 nm. Moreover, Fe_3O_4 NPs are congregated partially due to their large surface area and magnetic dipole-dipole interactions between particles [34].

Fig. 2B gives the XRD patterns for the Fe_3O_4 NPs and the CS–Fe_3O_4 nanocomposite. It indicates that Fe_3O_4 is the dominant component in both the samples. The characteristic peaks (2θ = 30.1°, 35.5°, 43.1°, 53.4°, 57.0°, 62.6°) of the two samples are marked by their indices ((2 2 0), (3 1 1), (4 0 0), (4 2 2), (5 1 1) and (4 4 0)). These peaks are consistent with the data in the database in JCPDS file (PDF No. 65-3107). Such results revealed that the resultant NPs were pure Fe_3O_4 with a spinel structure. It also suggested that the CS did not induce the phase change of Fe_3O_4.

X-ray photoelectron spectroscopy (XPS) experiments were carried out in order to verify the possible interaction between CS and Fe_3O_4, and the results were displayed in Fig. 3. The XPS spectrum of N (1s) in CS is at 398.99 eV (Fig. 3A), which could be ascribed to the carbon–nitrogen bond in CS. However, in the CS–Fe_3O_4 nanocomposite, there were two peaks at 398.46 eV and 400.27 eV, respectively (Fig. 3B), indicating that the N had two states in the nanocomposite. According to Fig. 3C and D, the XPS spectra of Fe (2p) changed from two characteristic bands (711.16 eV, 723.27 eV) in Fe_3O_4 NPs to four characteristic bands (710.96 eV, 714.09 eV, 721.28 eV, 724.82 eV) in the CS–Fe_3O_4 nanocomposite. The reason may be that the lone pair electrons of N atom in CS interact with the 3d orbital of Fe atom in Fe_3O_4 and hence forming a coordinate bond, which is consistent with the previous report [35].

3.2. Characterization of electrochemical behavior of CS–Fe_3O_4/GCE

Cyclic voltammetry (CV) of ferricyanide is an effective and convenient tool to monitor the surface status and the barrier of the modified electrode during each assembly step. Fig. 4A shows the CV responses of 5.0 mmol dm^{-3} $Fe(CN)_6^{3-/4-}$ at the bare GCE and the CS–Fe_3O_4/GCE respectively. As is shown, the electrochemical response for $Fe(CN)_6^{3-/4-}$ is a quasi-reversible process with the peak-to-peak separation of 87 mV at 100 mV s^{-1} at bare GCE (Fig. 4A, curve a). After modifying the electrode with CS–Fe_3O_4 nanocomposite, a significant increase in redox peak current is observed, which could be attributed to the large surface area of Fe_3O_4 NPs. Meanwhile, the peak-to-peak separation is increased (Fig. 4A, curve b), indicating that the nonconductive CS acts as an insulating layer and barriers which made the interfacial charge transfer inaccessible.

For further characterization of the modified electrode, electrochemical impedance spectroscopy (EIS) was employed to characterize the interfacial properties of the modified electrode using $Fe(CN)_6^{3-/4-}$ as the redox probe. Fig. 4B shows the impedance spectra in the form of Nyquist diagrams of bare GCE (Fig. 4B, curve a) and CS–Fe_3O_4/GCE (Fig. 4B, curve b). A small well defined semicircle (R_{ct} = 266 Ω) at higher frequencies was obtained at the bare GCE, suggesting a low transfer resistance. When CS–Fe_3O_4 nanocomposite was deposited on the GCE surface, the semicircle increased (R_{ct} = 727 Ω), indicating the impedance of the electrode increases in the presence of CS–Fe_3O_4 nanocomposite film, which obstructed the electron transfer of the $Fe(CN)_6^{3-/4-}$. This is because of the nonconductivity of chitosan in the film. These results demonstrated that CS–Fe_3O_4 nanocomposite was successfully immobilized on the GCE surface.

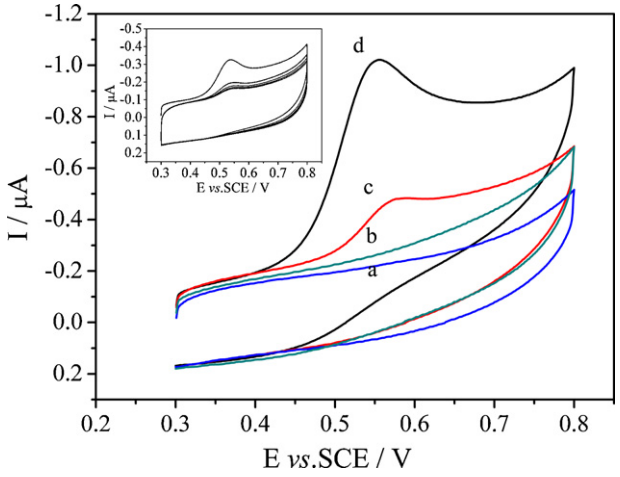

Fig. 5. Cyclic voltammograms recorded at first sweep of (a, b) 0 and (c, d) 1.0×10^{-5} mol dm^{-3} BPA at (a, c) GCE, (b, d) CS–Fe_3O_4/GCE in pH 8.0 PBS. Inset: progressive cyclic voltammograms for 2.5 μmol dm^{-3} BPA in pH 8.0 PBS. Scan rate: 100 mV s^{-1}. Accumulation time: 150 s. Accumulation potential: −0.1 V.

3.3. Electrochemical behavior of BPA at CS–Fe_3O_4/GCE

As shown in Fig. 5, the electrochemical responses of BPA at different electrodes were investigated using CV. When 1.0×10^{-5} mol dm^{-3} BPA was added into pH 8.0 PBS, only an oxidation peak is observed at both the electrodes within the potential window from 0.30 to 0.80 V. It revealed that the oxidation reaction of BPA is totally irreversible, which is in agreement with previous reports [21–23]. At the bare GCE (Fig. 5, curve c), the oxidation peak is observed at about 0.575 V with a low peak current. A significant enhancement in the anodic current was achieved with a low oxidation potential (0.541 V) at the modified electrode (Fig. 5, curve d), suggesting that the CS–Fe_3O_4 nanocomposite is an effective mediator in the electrocatalytic oxidation of BPA. In addition, compared with the GCE, the oxidation currents of BPA at the CS/GCE and the Fe_3O_4/GCE increased (not shown). Chitosan is a cationic polysaccharide with abundant amines, which has positive charges in the solution. Thus, we assumed that it was beneficial to absorb negatively charged BPA to enhance the current response. Fe_3O_4 NPs have the small dimension effect, the quantum size effect as well as the large surface area, which contributed to the significant improvement of the electrocatalytic activity of the modified electrode. Therefore, the current increase could be attributed to the synergetic activity of CS and Fe_3O_4, which lead to the larger electroactive surface of the modified electrode for the determination of BPA.

Moreover, it could be observed from inset of Fig. 5 that the anodic peak currents of BPA decrease significantly with the increase of the sweep number. The similar phenomenon was observed for other phenolic compounds [36]. This may be attributed to the fact

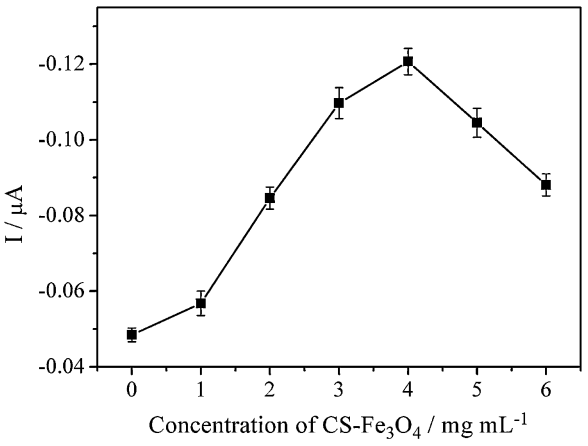

Fig. 6. Dependence of current response for 2.5 μmol dm^{-3} BPA oxidation on concentration of CS–Fe_3O_4. Other conditions are the same as Fig. 5.

that after the oxidation of BPA its oxidative product blocked the electrode surface [23]. Therefore, the oxidation signal during the first anodic sweep was recorded for BPA in the following studies.

The mechanism for electrochemical oxidation of phenolic compounds is a complex process. Although it is reported that direct oxidation of monophenolic compounds could generate o-quinone or p-quinone via four-electron and four-proton process [37], this process could be suppressed under the condition of low overpotential [38]. In our approach, one possible mechanism for the oxidation of BPA might be: (1) the formation of phenoxy radicals by losing electrons; (2) absorbance of phenoxy radicals on the surface of modified electrode; (3) the radicals could either be further oxidized to be quinones or couple with another radical to form dimeric products irreversibly, and/or, the generated quinones and phenoxy radicals undergo chemical reactions or a free radical multistep-growth polymerization to form various products through C–O, C–C and/or O–O coupling.

3.4. Optimization of the amount of the CS–Fe_3O_4

The optimization of the amount of CS–Fe_3O_4 on the surface of electrode has a predominant role on the voltammetric response for the oxidation of BPA. This can be controlled by using the same volume (10 μL) of the suspensions casted on the GCE surface with the different concentration of CS–Fe_3O_4. As can be observed from Fig. 6, the oxidation peak current for 2.5 μmol dm^{-3} BPA was increased by increasing the concentration of CS–Fe_3O_4 from 0 to 4 mg mL^{-1}. The further increase caused a gradual decrease in the anodic peak current of BPA, which could possibly be related to the increased film thickness. As a result, 10 μL of 4 mg mL^{-1} CS–Fe_3O_4 suspension was selected as the optimum volume for preparation of the modified electrode.

3.5. Effect of accumulation potential and time

It was believed that the significant enhancement of the current response of BPA on the modified electrode is partly attributed to the strong adsorption of the CS–Fe_3O_4 film on the GCE. Because the step of accumulation may increase the amount of BPA on the electrode surface, the accumulation under different potentials and times on the peak current in the solution with 2.5 μmol dm^{-3} BPA was studied by CV. As shown in Fig. 7A, the oxidation peak current increased remarkably when the accumulation potential was increased from −0.40 V to −0.10 V. However, with the further increase of the potential, the oxidation peak current decreased. Therefore, the accumulation potential was set at −0.10 V. It could be observed from Fig. 7B that the current increased gradually and reach a plateau with the accumulation time over 150 s. It indicated that, as the adsorptive equilibrium was reached, the amount of the adsorbed analyte is increased. With further increase of the accumulation time, the oxidation peak current increased slightly. So the accumulation time is set at 150 s.

3.6. Influence of the pH value and the potential scan rate

The effect of the pH value of the buffer solution on the electrochemical behavior of BPA was also studied. The investigations were preformed in the pH value ranging from 3.0 to 10.0 using 0.1 mol dm^{-3} PBS. It was found that the peak potential shifted negatively with the increase of the pH value and a good linear relationship was observed between the E_{pa} and pH values (Fig. 8, curve a) with the following equation:

$$E_{pa}\ (V) = -0.0524_{pH} + 0.993 \quad (R = 0.9917)$$

A value of about −52.4 mV per pH unit clearly indicates that equal numbers of electrons and protons are involved in the electrooxidation of BPA on the modified electrode [39]. Additionally, the oxidation peak current gradually increased with the increase of pH value from 3.0 to 8.0 (Fig. 8, curve b). The further increase of the pH value of the buffer solution made the current response decrease. The higher response to pH lower than the pK_a of BPA (pK_a = 9.73 [40]), suggests in this way that non-dissociated BPA can adsorbed better than the dissociated BPA on the surface of modified electrode [24,41]. Considering the sensitivity of the determination, PBS with the pH value of 8.0 was used as the supporting electrolyte in all voltammetric detection.

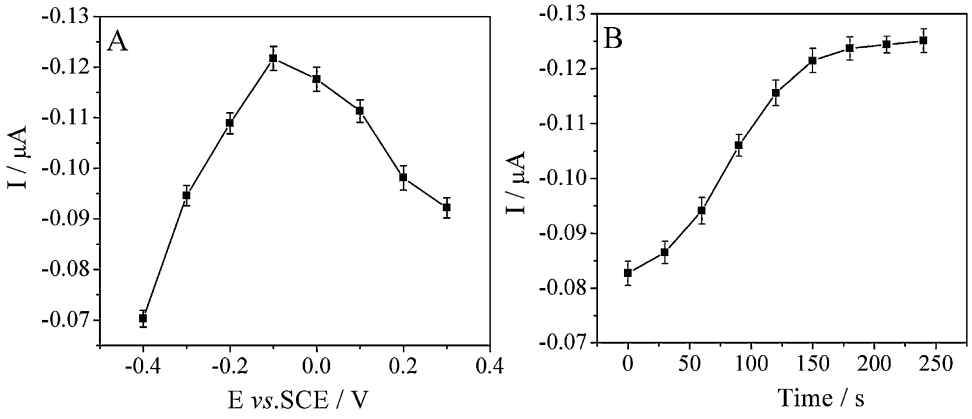

Fig. 7. Dependence of current response for 2.5 μmol dm^{-3} BPA oxidation on (A) accumulation potential and (B) accumulation time.

Table 1
Comparison of proposed sensor for determination of BPA with others.

Electrode	Linear range (μmol dm^{-3})	LOD (μmol dm^{-3})	Ref.
ITO	5–120	0.29	[21]
Thionine-tyrosinase/CPE[a]	0.15–45	0.15	[22]
CoPc-CPE	0.088–12.5	0.01	[23]
Poly-Ni(OH)NiTAPc/gold electrode	700–30,000	0.00368	[26]
MCM-41/CPE	0.088–0.22	0.038	[28]
MWCNT-GNPs/GCE	0.02–20	0.0075	[30]
tyrosinase/SWNT/CPE	0.1–12	0.02	[42]
Tyr[b]-SF[c]-MWNTs-CoPc/GCE	0.05–3.0	0.03	[43]
PAMAM[d]–Fe_3O_4/GCE	0.01–3.07	0.005	[44]
CS–Fe_3O_4/GCE	0.05–30	0.008	This work

[a] CPE: carbon paste electrode.
[b] Tyr: tyrosinase.
[c] SF: silk fibroin.
[d] PAMAM: poly (amidoamine).

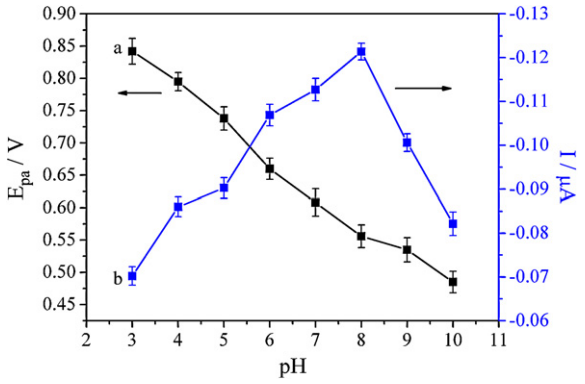

Fig. 8. Effects of pH value on the (a) current and (b) potential response of 2.5 μmol dm^{-3} BPA in 0.1 mol dm^{-3} PBS. Scan rate: 100 mV s^{-1}. Other conditions are the same.

The effect of the scan rate (v) on the oxidation of 2.5 μmol dm^{-3} BPA was investigated by CV with scan rate in the range from 20 to 700 mV s^{-1}. It is found that the relationship between the peak current of BPA and the scan rate is curvilinear (Fig. 9). Such results suggested that an adsorption process was involved in the electrochemical oxidation of BPA at CS–Fe_3O_4/GCE.

3.7. Differential pulse voltammetric determinations

As a highly sensitive and a low detection limit electrochemical method, differential pulse voltammetric (DPV) was used for the determination of BPA under the optimum conditions. Fig. 10A shows the DPV curves of BPA at the CS–Fe_3O_4/GCE at various concentrations. The oxidation peak currents are proportional to the concentration of BPA in a wider range of 5.0×10^{-8} to 3.0×10^{-5} mol dm^{-3}. The linear equation is I (μA) = −0.04717c (μmol dm^{-3}) −0.0021 (R = 0.9992), and the detection limit is as low as 8.0×10^{-9} mol dm^{-3} (S/N = 3) (Fig. 10B, curve a). By comparison, with the bare GCE, the linear range is only ranging from 1.5×10^{-7} to 8.7×10^{-6} mol dm^{-3} for BPA determination (Fig. 10B, curve b). With the increase of the BPA concentration to be 10.0 μmol dm^{-3}, the oxidation peak current began to decrease and change to zero quickly. The differences on the responses of BPA using the two kinds of electrodes suggested that the CS–Fe_3O_4 modified GCE is superior to the bare GCE on the determination of BPA.

As shown in Table 1, responses of the proposed method are compared with those obtained by other reported electrochemical methods. Our results are similar to those in the previous report using poly (amidoamine) for electrode fabrication [44]. The compared results indicated that the proposed method has the lower detection limit as well as wider linear range and could potentially be used to sensitively determine BPA.

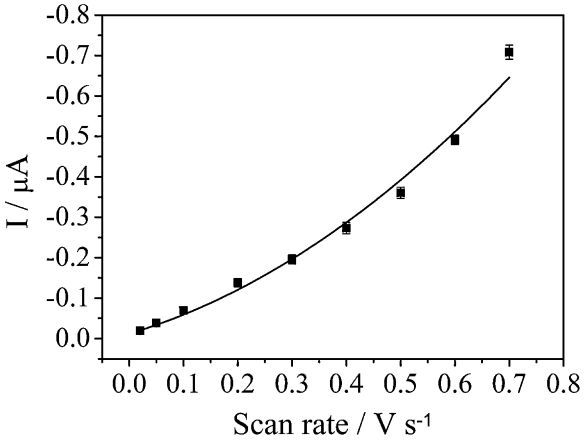

Fig. 9. The plot for the dependence of peak current of 2.5 μmol dm^{-3} BPA on the scan rate in 0.1 mol dm^{-3} pH 8.0 PBS. Other conditions are the same as Fig. 5.

3.8. Repeatability, stability and interference

The repeatability of the modified electrode was investigated by repetitively recording at a fixed BPA concentration of 2.5 μmol dm^{-3}. The relative standard deviation (RSD) for the oxidation peak currents with six determinations was 3.9%, indicating excellent repeatability of the modified electrode. Also, the electrode retained 93% of its initial peak current response after it was kept in

Table 2
Interferences of other species on 2.5 μmol dm^{-3} BPA.

Interferents	Concentration (mol dm^{-3})	I_{pa} change (%)
Ca^{2+}	2.5×10^{-4}	−3.1
Mg^{2+}	2.5×10^{-4}	−2.6
Zn^{2+}	2.5×10^{-4}	−4.0
Cu^{2+}	2.5×10^{-4}	+3.3
Fe^{3+}	2.5×10^{-4}	+4.5
Al^{3+}	2.5×10^{-4}	−3.9
SO_4^{2-}	2.5×10^{-4}	−2.0
NO_3^-	2.5×10^{-4}	−2.3
Phenol	1.25×10^{-4}	+5.2
Hydroquinone	1.25×10^{-4}	+4.5
Hydroxyphenol	1.25×10^{-4}	+5.0
Pyrocatechol	1.25×10^{-4}	−4.6
2-Nitrophenol	1.25×10^{-4}	+6.3
4-Nitrophenol	1.25×10^{-4}	+6.8
4-Chlorophenol	1.25×10^{-4}	+3.2
Ascorbic acid	5.0×10^{-5}	−4.7
Dopamine	5.0×10^{-5}	−5.2

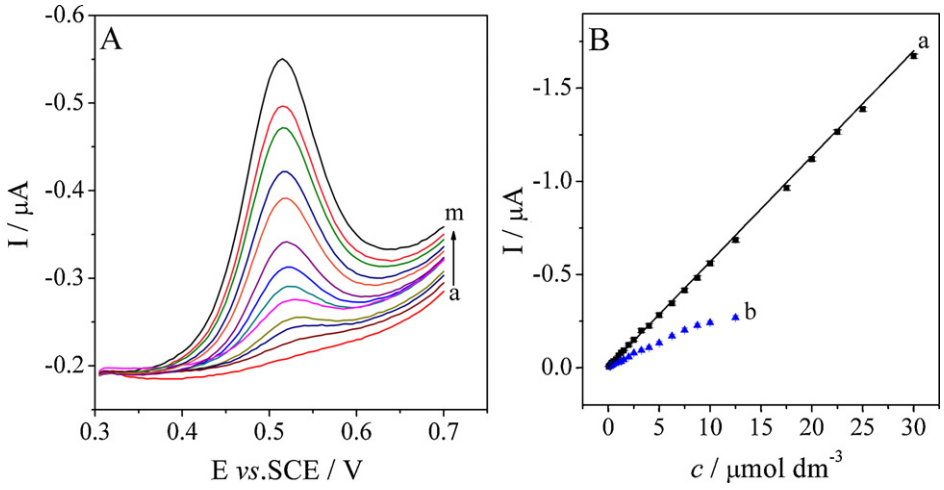

Fig. 10. (A) DPV curves of CS–Fe_3O_4/GCE in BPA solution at different concentrations (a–m): 0, 0.1, 0.35, 0.52, 0.75, 1.15, 1.55, 2.15, 3.05, 3.6, 4.55, 5.0, 5.95 μmol dm^{-3}. (B) Plot of the peak current against the concentration of BPA at (a) CS–Fe_3O_4/GCE and (b) GCE. Other conditions are the same as Fig. 5.

Table 3
Determination of BPA in plastic samples.

Sample	Measured (μmol dm^{-3})[a]	Added (μmol dm^{-3})	Found (μmol dm^{-3})[a]	RSD (%)	Recovery (%)
PVC drinking cup	1.23	1.25	2.52	3.11	101.6
PC nursing bottle	0.14	0.50	0.68	4.12	106.2
Baby's nipple	–	0.05	0.046	3.58	92.0
PVC food package	0.54	0.50	0.98	4.27	94.2

[a] Mean of five measurements.

refrigerator at 4 °C for two weeks, which shows long-term stability of the CS–Fe_3O_4 film on the GCE surface.

The influences of common interfering species on the determination of BPA were investigated in the presence of 2.5 μmol dm^{-3} BPA with great details. The results are listed in Table 2. It is found that lots of species almost have no influence on the peak current, suggesting that the proposed method has excellent selectivity toward BPA.

3.9. Application to real sample analysis

In order to evaluate the performance of the CS–Fe_3O_4/GCE in practical analytical applications, the proposed method was used to detect BPA in different plastic samples under optimized conditions. A known-amount of sample solution was added into pH 8.0 PBS, and then analyzed according to the above procedure. Each sample solution undergoes five parallel determinations. The data given in Table 3 indicated that our approach could provide satisfactory results for the determination of BPA.

3.10. BPA leaching experiments

We studied the influence of incubation time on BPA leaching in water at neutral pH using the proposed method. As shown in Fig. 11, the average BPA concentration obtained from new drinking cups increased gradually with the incubation time increased from 2 days to 6 days at 40 °C. When the temperature increased to be 55 °C, the BPA concentration increased remarkably with the increase of incubation time. Our data agreed well with the results obtained by Le et al. [45]. In their study it was observed that the released BPA from PC bottles at room temperature increased via time. Combined with Table 3, our investigation with our approach demonstrated that both temperature and time are critical factors for BPA leaching to water. The conditions of higher temperature and longer incubation time resulted in higher BPA from the testing samples.

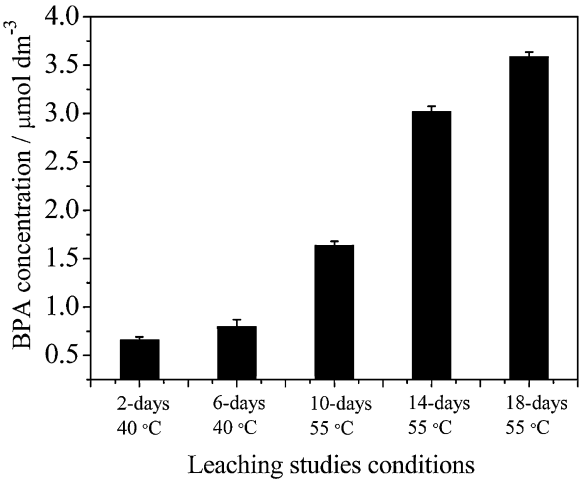

Fig. 11. Average concentration of BPA (mean of five measurements) leached from new drinking cups in water.

4. Conclusions

In this work, we demonstrated that the modification of GCE with CS–Fe_3O_4 nanocomposite is effective for the highly sensitive determination of BPA. CS–Fe_3O_4 nanocomposite could remarkably enhance the response and decrease its oxidation overpotential. The electrochemical behavior of BPA at the CS–Fe_3O_4 is an absorption-controlled process involving equal numbers of electrons and protons. The responses of CS–Fe_3O_4/GCE toward the practical determination of BPA were studied. The wider linear range, the lower detection limit, the better stability and repeatability, and the higher sensitivity of this approach demonstrated that it is

promising for the efficient amperometric determination of BPA. Additionally, the leaching study indicated that the amount of BPA releasing increased with the increase of incubation time. In our future work, we will try to integrate microchip electrophoresis to explore the possibility of multianalyte detection using our modified electrode.

Acknowledgements

This work was financially supported by the National Natural Science Foundation of China (Grant numbers: 81001263, 20875051, 20675042 and 21075070), the Natural Science Foundation of Jiangsu Province (Grant number: BK2009152), the Universities Natural Science Foundation of Jiangsu Province (Grant number: 10KJB150015).

References

[1] C.A. Staples, P.B. Dome, G.M. Klecka, S.T. Oblock, L.R. Harris, Chemosphere 36 (1998) 2149.
[2] Y. Mutou, Y. Ibuki, Y. Terao, S. Kojima, R. Goto, Environ. Toxicol. Pharmacol. 21 (2006) 283.
[3] K.L. Howdeshell, P.H. Peterman, B.M. Judy, J.A. Taylor, C.E. Orazio, R.L. Ruhlen, F.S.V. Saal, W.V. Welshons, Environ. Health Perspect. 111 (2003) 1180.
[4] H. Segner, J.M. Navas, C. Schäfers, A. Wenzel, Ecotoxicol. Environ. Saf. 54 (2003) 15.
[5] C.A. Staples, J.W. Davis, Chemosphere 49 (2002) 61.
[6] Y. Nakagawa, T. Suzuki, S. Tayama, Toxicology 156 (2000) 27.
[7] R. Steinmetz, N.A. Mitchner, A. Grant, D.L. Allen, R.M. Bigsby, N. Ben-Jonathan, Endocrinology 139 (1998) 2741.
[8] M.C. Estevez, R. Galve, F. Sanchez-Baeza, M.P. Marco, Anal. Chem. 77 (2005) 5283.
[9] C. Lu, J.G. Li, Y. Yang, J.M. Lin, Talanta 82 (2010) 1576.
[10] K. Inoue, K. Kato, Y. Yoshimura, T. Makino, H. Nakazawa, J. Chromatogr. B 749 (2000) 17.
[11] M. Liu, Y. Hashi, F. Pan, J. Yao, G. Song, J. Lin, J. Chromatogr. A 1133 (2006) 142.
[12] R.J.W. Meesters, H.F. Schroder, Anal. Chem. 74 (2002) 3566.
[13] S.C. Cunha, J.O. Fernandes, Talanta 83 (2010) 117.
[14] S. Berkner, G. Streck, R. Herrmann, Chemosphere 54 (2004) 75.
[15] J. Roger, S. Hassan, S. Emmanuel, D. Thierry, D. Katja, J. Chromatogr. A 974 (2002) 143.
[16] K.R. Rogers, J.Y. Becker, J. Wang, F. Lu, Field Anal. Chem. Technol. 3 (1999) 161.
[17] M.M. Ngundi, O.A. Sadik, T. Yamagushi, S.I. Suye, Electrochem. Commun. 5 (2003) 61.
[18] H. Kuramitz, J. Saitoh, T. Hattori, S. Tanaka, Water Res. 36 (2002) 3323.
[19] H.S. Yin, Y.L. Zhou, S.Y. Ai, R.X. Han, T.T. Tang, L.S. Zhu, Microchim. Acta 170 (2010) 99.
[20] D. Vega, L. Agüí, A. González-Cortés, P. Yáñez-Sedeño, J.M. Pingarrón, Talanta 71 (2007) 1031.
[21] Q. Li, H. Li, G.F. Du, Z.H. Xu, J. Hazard. Mater. 180 (2010) 703.
[22] M. Portaccio, D.D. Tuoro, F. Arduini, M. Lepore, D.G. Mita, N. Diano, L. Mita, D. Moscone, Biosens. Bioelectron. 25 (2010) 2003.
[23] H.S. Yin, Y.L. Zhou, S.Y. Ai, J. Electroanal. Chem. 626 (2009) 80.
[24] H.S. Yin, L. Cui, S.Y. Ai, H. Fan, L.S. Zhu, Electrochim. Acta 55 (2010) 603.
[25] E. Dempsey, D. Diamond, A. Collier, Biosens. Bioelectron. 20 (2004) 367.
[26] V. Chauke, F. Matemadombo, T. Nyokong, J. Hazard. Mater. 178 (2010) 180.
[27] H.S. Yin, Y.L. Zhou, S.Y. Ai, Q.P. Chen, X.B. Zhu, X.G. Liu, L.S. Zhu, J. Hazard. Mater. 174 (2010) 236.
[28] F.R. Wang, J.Q. Yang, K.B. Wu, Anal. Chim. Acta 638 (2009) 23.
[29] J.D. Huang, X.M. Zhang, Q. Lin, X.R. He, X.R. Xing, H.X. Huai, W.J. Lian, H. Zhu, Food Control 22 (2011) 786.
[30] X.M. Tu, L.S. Yan, X.B. Luo, S.L. Luo, Q.J. Xie, Electroanalysis 22 (2009) 2491.
[31] S.F. Wang, Y.M. Tan, D.M. Zhao, G.D. Liu, Biosens. Bioelectron. 23 (2008) 1781.
[32] Y.C. Chang, D.H. Chen, J. Colloid Interface Sci. 283 (2005) 446.
[33] T.T. Pham, C. Cao, S.J. Sim, J. Magn. Magn. Mater. 320 (2008) 2049.
[34] K.R. Reddy, K.P. Lee, A.G. Lyengar, J. Appl. Polym. Sci. 104 (2007) 4127.
[35] J.G. Deng, Y.X. Peng, C.L. He, X.P. Long, P. Li, A.S.C. Chan, Polym. Int. 52 (2003) 1182.
[36] J. Wang, S.P. Chen, M.S. Lin, J. Electroanal. Chem. 273 (1989) 231.
[37] M. Ferreira, H. Varela, R.M. Torresi, G. Tremiliosi-Filho, Electrochim. Acta 52 (2006) 434.
[38] L. Papouchado, R.W. Sandford, G. Petrie, R.N. Adams, J. Electroanal. Chem. 65 (1975) 275.
[39] T. Luckza, Electrochim. Acta 53 (2008) 5725.
[40] H. Sambe, K. Hoshina, K. Hosoya, J. Haginaka, J. Chromatogr. A 1134 (2006) 16.
[41] L. Fernández, C. Borrás, H. Carrero, Electrochim. Acta 52 (2006) 872.
[42] D.G. Mita, A. Attanasio, F. Arduini, N. Diano, V. Grano, U. Bencivenga, S. Rossi, A. Amine, D. Moscone, Biosens. Bioelectron. 23 (2007) 60.
[43] H.S. Yin, Y.L. Zhou, J. Xu, S.Y. Ai, L. Cui, L.S. Zhu, Anal. Chim. Acta 659 (2010) 144.
[44] H.S. Yin, L. Cui, Q.P. Chen, W.J. Shi, S.Y. Ai, L.S. Zhu, L.N. Lu, Food Chem. 125 (2011) 1097.
[45] H.H. Le, E.M. Carlson, J.P. Chue, S.M. Belcher, Toxicol. Lett. 176 (2008) 149.